Original Article

Evaluation of Low-dose Computed Tomography Images Reconstructed Using Artificial Intelligence-based Adaptive Filtering for Denoising: A Comparison with Computed Tomography Reconstructed with Iterative Reconstruction Algorithm

Suyash Kulkarni, Vasundhara Patil, Aniruddha Nene[1], Nitin Shetty, Amitkumar Choudhari, Akansha Joshi, CS Pramesh[2], Akshay Baheti, Kalpesh Mahadik

Department of Radiodiagnosis, Tata Memorial Hospital, Homi Bhabha National Institute, [1]Graone Solutions Pvt. Ltd., Kalyan, One Sg Technologies Pvt. Ltd., Pune, Maharashtra, India, [2]Department of Thoracic Surgery, Tata Memorial Hospital, Homi Bhabha National Institute, Mumbai, India

Abstract

Purpose: Awareness of radiation-induced risk led to the development of various dose optimization techniques in iterative reconstruction (IR) algorithms and deep learning algorithms to improve low-dose image quality. PixelShine (PS) by AlgoMedica Inc., USA, is a vendor-neutral deep learning denoising tool for low-dose studies, and this study analyzed its images. **Aim:** The aim of this study was to assess the diagnostic value of PS-reconstructed images obtained at various low doses (LDs). **Materials and Methods:** A retrospective study qualitatively and quantitatively evaluated the low-dose PS-reconstructed images by comparing them with other reconstruction methods and standard dose (SD) images. A total of 85 cases were evaluated, of which 32 cases were scanned on a scanner with filtered back projection (FBP) reconstruction with LD scans performed at 70%–50% of SD. The remaining 53 cases were performed on the scanner with IR, 35 of them had LD scan at 50% of SD and 18 cases had LD scan at 33% of SD. **Results:** Qualitative image analysis – The quality of low-dose images with PS and IR was almost equivalent in terms of noise magnitude and texture at 50% dose, and PS images were slightly better at 33% dose reduction. Quantitative image analysis – Low-dose PS-reconstructed images and low-dose iterative reconstructed images had similar contrast-to-noise ratio at 50% dose reduction; however, at 33% of the SD, PS-reconstructed images outperformed. The SD FBP images were equivalent to LD PS-reconstructed images (50% dose reduction). **Conclusions:** Artificial intelligence-based denoising algorithms produce similar images as IR at 50% dose reduction and outperform it at 33% of the SD.

Keywords: Artificial intelligence-based denoising image reconstruction algorithm, low-dose computed tomography images, PixelShine

Received on: 10-07-2024 **Review completed on: 06-11-2024** **Accepted on: 10-01-2025** **Published on: 24-03-2025**

Introduction

The last decade witnessed an increase in the awareness about radiation-induced risk sustained during medical imaging procedures of computed tomography (CT) scan.[1] This led to the development of various dose optimization techniques to improve image quality at lower radiation doses. The benefits of low-dose imaging are not only limited to patient safety but also increase the X-ray tube life due to lower dissipation of the tube energy. The energy saving benefits the facility and is a step toward sustainable diagnostic care.

However, the main limitation while reducing CT dose is the resulting increase in the image noise, and this necessitates the processing for noise reduction. Recent advances have been made in both iterative reconstruction (IR) algorithms and a

Address for correspondence: Dr. Suyash Kulkarni, Department of Radiodiagnosis, Tata Memorial Hospital, Dr. Ernest Borges Marg, Parel East, Mumbai - 400 012, Maharashtra, India.
E-mail: suyashkulkarni@yahoo.com

Access this article online

Quick Response Code:

Website: www.jmp.org.in

DOI: 10.4103/jmp.jmp_115_24

How to cite this article: Kulkarni S, Patil V, Nene A, Shetty N, Choudhari A, Joshi A, *et al*. Evaluation of low-dose computed tomography images reconstructed using artificial intelligence-based adaptive filtering for denoising: A comparison with computed tomography reconstructed with iterative reconstruction algorithm. J Med Phys 2025;50:108-17.

new deep learning/artificial intelligence (AI)-based algorithm to provide substantial image noise reduction.

In a CT scanner, after the acquisition of the X-ray projection data by the detectors in the machine, various reconstruction techniques are used to process these data to form the image. Filtered back projection (FBP) followed by IR has been commonly implemented to reconstruct CT images. IR is presently used in scanners for CT image reconstruction. IR also witnessed advancement, and different generations of the IR algorithm were developed.[2] The IR techniques are by large proprietary and native to the console. Therefore, the comparison of different IRs used by vendors is not straightforward. One cannot use the data of one CT modality and use the same on multiple standalone IR workstations easily. Such comparison usually requires repeated scans on different CT models with identical exposure. CT modalities themselves have different inherent hardware advantages, such as the latest detector technology that provides a higher sensitivity to radiation and hence can operate at a lower dose than their older generation counterparts.[3] Some CT scanners modulate the exposure in certain regions of interest, during the scan, by accurately controlling input energy to the tube.[4] Therefore, a comparison of the performance of any algorithm must take into consideration these aspects.

Significant advancement in medical imaging also witnessed the development of machine learning-based sophisticated algorithms (AI). PixelShine® by AlgoMedica Inc., USA, is one of such vendor-neutral tools that was used for the assessment of digital techniques for denoising the low-dose (LD) studies. It is a US-patented product, commercially available as a perpetual license or annual subscription. It uses the deep learning for denoising the CT scans.[5,6] This deep learning type of algorithm initiates a new concept regarding image quality optimization by denoising and is completely different from the current IR algorithm.[7-9]

This study aims to assess the diagnostic value of images obtained by PixelShine (PS) acquired at LD and compare them with other reconstruction techniques available. It also attempts to establish the extent of dose reduction obtained without losing the required diagnostic level.

The Indian Perspective

A substantial number of CT scanners in India do not have the IR module because IR is more relevant when the dose is low and the noise is high. In the absence of any firm guideline from the regulatory authorities on the usage of IR or other algorithms to reduce exposure, and because of the general lack of awareness, the diagnostic ecosystem tends to continue with standard protocols despite the possibility of employing low-dose acquisition and processing techniques.

CT vendors offer IR as an optional module and a substantial number of CT scanners installed in India did not opt for this module. A large chunk of CT scan installations in India represents the older generation of/refurbished models of CT scanners that do not have the IR module. As the IR module is not a vendor-neutral plugin, for the older CT scanners, upgradation to IR-compatible console is either not feasible or turns out to be very expensive.

Considering these facts, the study also included data acquired from a CT scanner that did not have an IR module. The comparison in this was possible with the baseline reconstruction FBP itself and AI-driven tools such as PS. The outcome on noise reduction was expected to be obviously in favor of the AI technique, but the purpose was to establish the level of dose reduction that can be established using AI techniques for both possibilities: with/without IR module. When the IR module is available, the study provides a comparison of performance. The assessment was done using subjective and objective methodologies.

Acquisition of the Computed Tomography-guided Biopsy Data

This retrospective study evaluated the diagnostic value of the low-dose CT images reconstructed by the three methods – FBP, IR and PS. The study included the images obtained during the CT-guided biopsy procedure performed in the department. In a CT-guided biopsy procedure, there is a need to scan the patient multiple times which leads to high radiation doses. The CT biopsy protocols can be divided into three phases of image acquisition – the planning phase, the targeting phase, and the postprocedure phase. Each phase has different aims and hence different diagnostic image quality expectations. The first or the planning phase of biopsy often needs to be of a diagnostic quality. The dose reduction is not performed at this stage as it would compromise the primary diagnosis and is performed as per the institute's established protocol. The second targeting phase needs multiple acquisitions to localize/guide the needle and acquire samples. In this phase, the diagnostic aspect of the image is less of a concern and is required mainly for needle localization or guidance. Low-dose protocols are specifically recommended for this phase of acquisition.[10-12] The postprocedure phase is performed to exclude any complications and may need a diagnostic or low-dose image depending on the site of the biopsy.

LD protocols specifically configured for targeting and postprocedure phase as per institute protocol were selected. The low-dose protocols provided alternatives of 70%, 50%, and 33% doses as compared to the dose in the planning phase (100%). The extent of the LD was a parameter for the study, and LD cases were selected.

These low-dose images obtained from the biopsy procedures were postprocessed and evaluated concerning their diagnostic quality and noise.

The baseline data or FBP image series generated by the CT models for the targeting phase of the biopsy was in turn further processed by proprietary IR algorithm native to the console (if available) and PS, AI-driven algorithm.

This effectively eliminates the influence of hardware features of individual CT models that could affect the outcomes and ensures that the acquisition parameters for both methods are the same to have a fair comparison purely of the efficacy of the two algorithms above. In case the CT scan has no native IR module available, PS algorithm was applied to FBP images to confirm the retention of the diagnostic quality of the images processed using AI.

Material and Methods

This was an Institutional Review Board-approved retrospective study, and the requirement of patients' informed consent was waived. The hospital record was searched to identify adult patients who underwent CT-guided biopsy in the institute between January 2022 and September 2023. The institute protocol was set to perform the planning phase of the CT scan at a standard dose (SD). The needle localization phase was performed at an LD.

Images were archived on Centricity PACS (GE HealthCare) and reviewed. The cases were included in the study whose planning phase scan was performed at the SD and at least one CT scan acquisition was performed at an LD, i.e. lower mA compared to the standard protocol without changing the kV, and raw data, i.e., FBP images were available. The low-dose images were sent to the PS postprocessing server using DICOM connectivity.

Approximately 660 patients who underwent CT-guided biopsy procedures in the department were screened and their radiation dose and sequences were studied. Eighty-five adult patients were identified as having at least one sequence performed at SD and at least one at LD during the procedure, and FBP data were available on the console.

Computed Tomography Acquisition Protocols and Specifications

The CT examinations were performed on two scanners.

Scanner A- 16 Slice Siemens Open CT scanner model – Sensation with Care Dose feature and CT-guided intervention-specific protocols and tools. The native IR was not available.

32 cases were identified retrospectively having a study with SD series as well as an LD series up to 70%–50% of the SD level. The LD was not a specific fixed % of the SD and ranged from 70% to 50% of SD.

Scanner B-128 Slice, "Incisive" CT model by Philips HealthCare enabled with ultra-LD/70 kV scan protocols, 3D dose modulation with DRI, Latest Elite digital detector technology, 1 to 7 level iterations with iDose 4 technology. Dose modulation was used for the SD protocol, whereas uniform/fixed dose reduction strength was used for the LD protocol.

Fifty-three cases were identified retrospectively with SD-IR, 35 cases had a series with 50% of the SD and 18 cases had a series with 33% of the SD.

The SD axial images were used as the benchmark for quality. The series with LD-CT acquisition in FBP were postprocessed using the PS AI algorithm (LD-PS) at the local server (for both scanner A and B above) and also with iDose IR (LD-IR), only in the cases of scanner B. In addition, the LD images reconstructed with FBP (LD-FBP) were available for comparison, and the results were analyzed qualitatively and quantitatively.

Assessment and image analysis

Two radiologists with one with 20 years of experience and another with 4 years of experience in radiology reviewed the images in consensus. The LD-PS images were compared with the SD images acquired during the planning phase of biopsy (for retention of the diagnostic quality) and LD scans during the targeting phase obtained after FBP or IR.

Five qualitative aspects of the image quality were subjectively analyzed with respect to its diagnostic quality. These were noise magnitude, noise texture, edge sharpness, artifacts, and overall diagnostic quality. A score of 1–5, up to one decimal point, was assigned on subjective analysis for each of these parameters, and a final score was calculated from them.

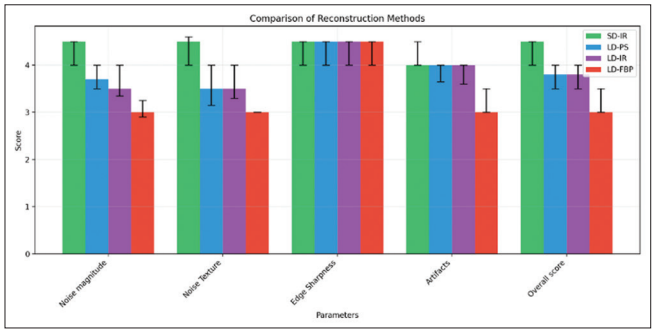

Figure 1: Bar diagram with interquartile ranges depicting qualitative results of the parameters of the images (n = 35) obtained by scanner B with native iterative reconstruction – iDose: at low dose LD = 1/2 or 50% of standard dose. SD: Standard dose, IR: Iterative reconstruction, LD: Low dose, PS: PixelShine, FEB: Filtered back projection

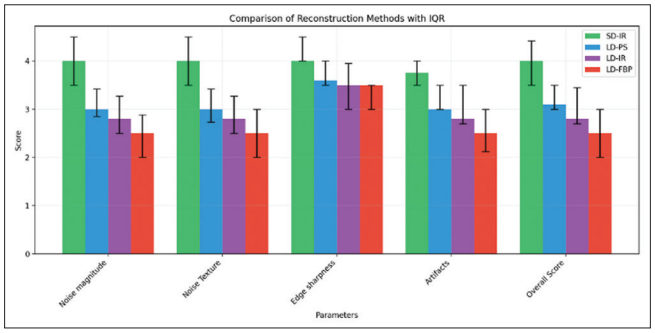

Figure 2: Bar diagram with interquartile ranges depicting qualitative results of the parameters of the images (n = 18) obtained by scanner B with native iterative reconstruction – iDose: at low dose = 1/3 or 33% of standard dose. SD: Standard dose, IR: Iterative reconstruction, LD: Low dose, PS: PixelShine, FEB: Filtered back projection, IQR: Interquartile range

Standards for evaluation used were: (1) unacceptable, (2) suboptimal but acceptable, (3) average, (4) good, and (5) excellent.

A subjective score >3 points indicated that the image fulfilled the clinical requirements.

For quantitative analysis, ROI measurements were performed on muscle in a field of view that was relatively homogeneous. Circular ROIs of approximately 2.0 cm^2 were drawn on at least 3 consecutive image slices on the muscle and lateral airspace for background measurements. The ROI was drawn on the same slice of planning scan, LD scan with IR, and LD scan with PS reconstruction. CT densities value was calculated in Hounsfield unit (HU) value in soft window (350 and 50). The noise was assessed as HUs and standard deviation within the region of interest selected, i.e., muscle.

Image quality calculations: Signal-to-noise ratios (SNRs) and contrast-to-noise ratios (CNRs) were calculated.

SNR is commonly used to quantify image noise and is defined as the mean attenuation of the ROI divided by its standard deviation.[9,13-15]

SNR = Mean HU (muscle)/SD HU (muscle)

CNR reflects the effect of noise on the image. The CNR is defined as the difference in the mean attenuation in the ROI and the lateral airspace ROI divided by the square root of the sum of their variances:

CNR= (Mean HU [muscle] – Mean HU [air])/root of (SD muscle^2 + SD air^2)/2

The kV and mA of the image were also noted, and a percentage reduction in mA was calculated. The study was analyzed statically.

Statistical Analysis and Results

The median values obtained from the qualitative and quantitative analysis are shown in the form of bar diagrams with interquartile range in Figures 1-7.

Qualitative Image Analysis Results

Noise magnitude and texture

At 33% and 50% of original mA, the image quality of LD-PS images in terms of noise magnitude and texture was lower than SD-IR and better than LD-FBP with a significant

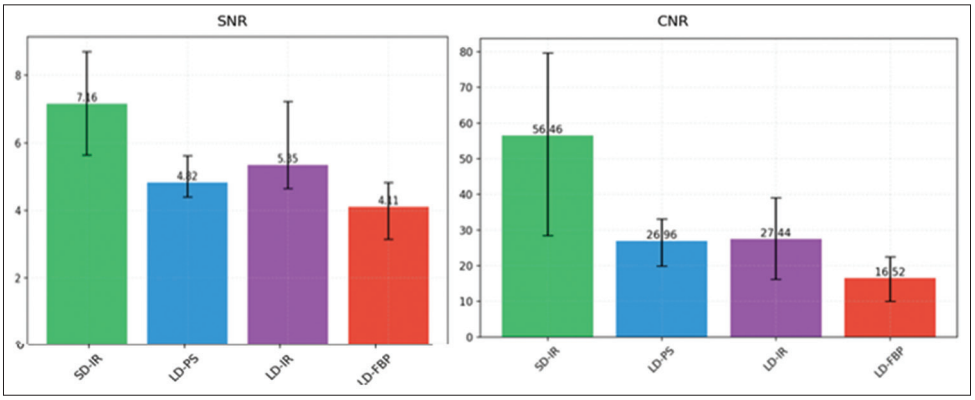

Figure 3: Bar diagram with interquartile ranges depicting quantitative results of the parameters of the images (n = 35) obtained by Scanner B with native iterative reconstruction – iDose: A at low dose = 1/2 or 50% of standard dose. SD: Standard dose, IR: Iterative reconstruction, LD: Low dose, PS: PixelShine, FEB: Filtered back projection, SNR: Signal-to-noise ratio, CNR: Contrast-to-noise ratio

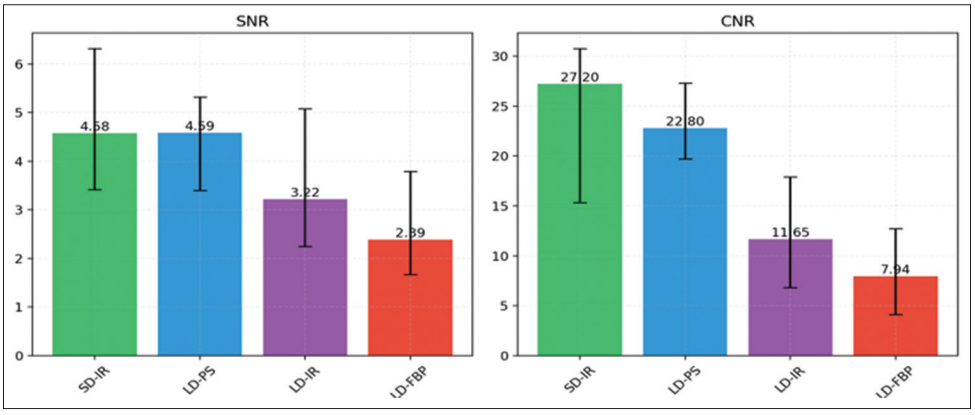

Figure 4: Bar diagram with interquartile ranges depicting quantitative results of the parameters of the images (n = 18) obtained by Scanner B with native iterative reconstruction – iDose: A at low dose = 1/3 or 33% of standard dose. SD: Standard dose, IR: Iterative reconstruction, LD: Low dose, PS: PixelShine, FEB: Filtered back projection, SNR: Signal-to-noise ratio, CNR: Contrast-to-noise ratio

P value [Figures 1 and 2]. The LD-PS images were almost equivalent to LD-IR at 50% dose and slightly better at 33% dose with *P* value, as given in Table 1. At 50-70% dose reduction the image quality in terms of noise magnitude and texture was lower in SD-IR than SD-FBP with significant p value for noise magnitude [Figure 6 and Table 2].

Edge sharpness

The edge sharpness of images at SD-IR, LD-PS, LD-IR, and LD-FBP was similar at 50% dose reduction [*P* value not significant, Table 1]. At 33% of SD, the edge sharpness was similar in LD-PS images and LD-IR images, thus margins were not compromised [Figures 1 and 2]. The edge sharpness of PS images was less than SD-FBP ($P = 0.001$) [Figure 6 and Table 2]. The edge sharpness of LD-PS was more than LD-FBP with $P = 0.021$ [Table 2].

Artifacts

The artifacts were slightly less in PS-reconstructed images than in IR (at LD, more marked at 33% dose than 50%); however, the *P* value was not significant [Figures 1, 2 and 6]. Compared to the PS-reconstructed images, more artifacts were seen in the FBP-reconstructed images ($P < 0.001$). The SD images had fewer artifacts than all low-dose images with any reconstruction ($P < 0.001$).

Overall score

At 50% mA reduction, the median score of LD-PS-reconstructed images and LD-IR images was the same, and the *P* value was not significant. However, at 33% of SD mA, PS-reconstructed images were superior to IR images with significant *P* value. The overall score was significantly higher for SD-IR and SD-FBP compared to LD-PS images at all dose reduction, however, the mean/median bias was 0.63 (−0.31, 1.57) and 0.5 (−0.07, 1.87) respectively and 6% points were outside the Bias confidence limits [Table 3] for scanner B and the mean/median bias for scanner A was 0.34 (-0.84-1.53) and 3% points were outside the bias confidence limits [Table 4].

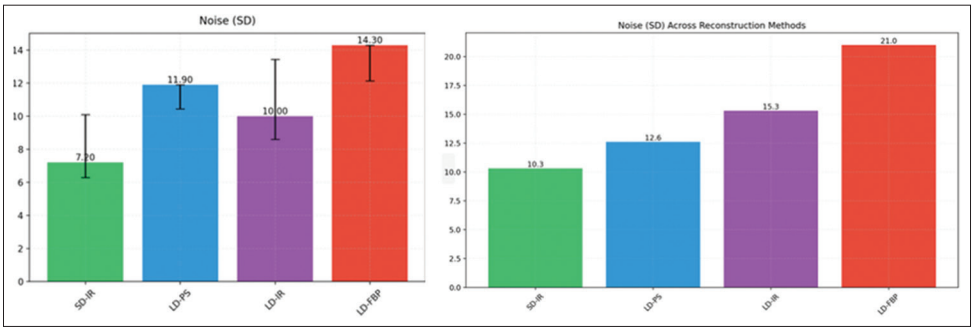

Figure 5: Bar diagram with interquartile ranges showing noise obtained by Scanner B with native iterative reconstruction – iDose: at 50% of standard dose (SD) (left) and 33% of SD (right). SD: Standard dose, IR: Iterative reconstruction, LD: Low dose, PS: PixelShine, FEB: Filtered back projection

Table 1: The *P*-value of standard dose-iterative reconstruction versus low dose-PixelShine, low dose-PixelShine versus low dose-iterative reconstruction, and low dose-PixelShine versus low dose-filtered back projection images (using paired *t*-test or Wilcoxon signed-rank test) obtained from the analysis of the image of Scanner B with native iterative reconstruction – iDose ($n=53$)

Dose (percentage of SD mA)	Variable	Test (*P*)		
		SD-IR versus LD-PS	LD-PS versus LD-IR	LD-PS versus LD-FBP
33	Noise magnitude	0.000	0.038	0.000
50	Noise magnitude	0.000	0.826	0.000
33	Noise texture	0.000	0.083	0.000
50	Noise texture	0.000	0.634	0.000
33	Edge sharpness	0.001	0.097	0.021
50	Edge sharpness	0.172	0.497	0.135
33	Artifacts	0.000	0.073	0.000
50	Artifacts	0.001	0.085	0.001
33	Overall score	0.000	0.005	0.000
50	Overall score	0.000	0.806	0.000
33	SNR	0.108	0.015	0.000
50	SNR	0.000	0.002	0.000
33	CNR	0.833	0.000	0.000
50	CNR	0.000	0.442	0.000

SD: Standard dose, LD: Low dose, IR: Iterative reconstruction, PS: PixelShine, FBP: Filtered back projection, SNR: Signal-to-noise ratio, CNR: Contrast-to-noise ratio

Quantitative image analysis results

SNR and CNR were higher in SD-IR images than in LD-PS images at 50% mA reduction with significant *P* value [Figures 3 and 4]. However, when the dose was reduced to 33% of the original mA, PS images were comparable with SD-IR images and the difference was not significant (*P* value of 0.108 for SNR and 0.833 for CNR). LD-PS-reconstructed images compared to LD-IR images had similar CNR at 50% dose reduction but less SNR [Figure 3]. However, when the dose was reduced to 33% of SD, the CNR and SNR of PS-reconstructed images were higher than LD-IR images [Figure 4].

Table 2: The *P*-value of standard dose-filtered back projection versus low dose-PixelShine, and low dose-PixelShine versus low dose-filtered back projection images (using paired *t*-test or Wilcoxon signed-rank test obtained from the analysis of the image of Scanner A without any native iterative reconstruction (*n*=32)

Dose (percentage of SD mA)	Variable	Test (*P*)	
		SD-FBP versus LD-PS	LD-PS versus LD-FBP
50–70	Noise magnitude	0.041	0.000
50–70	Noise texture	0.100	0.000
50–70	Edge sharpness	0.001	0.791
50–70	Artifacts	0.015	0.001
50–70	Overall score	0.003	0.000
50–70	SNR	0.933	0.037
50–70	CNR	0.856	0.051

SD: Standard dose, LD: Low dose, PS: PixelShine, FBP: Filtered back projection, SNR: Signal-to-noise ratio, CNR: Contrast-to-noise ratio

Compared to SD-FBP-reconstructed images, the LD-PS-reconstructed images had similar CNR and SNR (*P* value not significant) [Table 2 and Figure 7].

Noise

Image noise is defined as SD in HU value in muscle. The noise in the image was lowest for SD, followed by PS and FBP. At 50% dose reduction, noise however was lower in IR than PS-reconstructed images, but at further dose reduction to 30%, PS images had less noise than IR images.

Discussion

This retrospective study qualitatively and quantitatively evaluated the image quality of the deep learning-based image denoising reconstruction technique of low-dose scans obtained on two scanners and compared it with other reconstruction techniques.

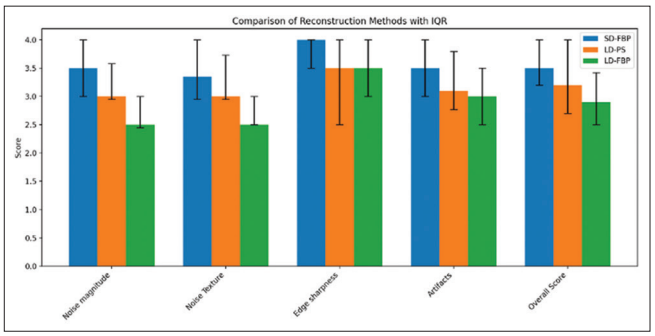

Figure 6: The qualitative results of the parameters of the images (*n* = 32) obtained by Scanner A without any native iterative reconstruction. Dose low dose = Ranged from 70% to 50% of standard dose. SD: Standard dose, FEP: Filtered back projection, LD: Low dose, PS: PixelShine, IQR: Interquartile range

Table 3: The mean/median bias and points outside bias confidence interval limits in comparison of standard dose-iterative reconstruction versus low dose-PixelShine, and low dose-PixelShine versus low dose- iterative reconstruction images (obtained from Scanner B with native iterative reconstruction – iDose, *n*=53)

Dose (percentage of SD mA)	Variable	SD-IR versus LD-PS		LD-PS versus LD-IR	
		Mean/median bias (bias CL)	Percentage points outside bias CL	Mean/median bias (bias CL)	Percentage points outside bias CL
33	Noise magnitude	0.85 (0.09–1.61)	6	0.19 (−0.52–0.91)	6
50	Noise magnitude	0.5 (0–1.54)	3	0 (−0.58–1.18)	6
33	Noise texture	0.87 (0.03–1.7)	6	0.15 (−0.53–0.83)	6
50	Noise texture	0.5 (−0.07–2.3)	6	0 (−0.95–0.83)	6
33	Edge sharpness	0.5 (−0.12–1.29)	11	0.19 (−0.73–1.11)	0
50	Edge sharpness	−0.2 (−1–1.6)	3	0 (−1.6–1)	3
33	Artifacts	0.52 (−0.36–1.4)	6	0.18 (−0.6–0.95)	11
50	Artifacts	0.5 (−0.58–1.45)	6	0 (−1.19–1.07)	6
33	Overall score	0.63 (−0.31–1.57)	6	0.25 (−0.5–1)	6
50	Overall score	0.5 (−0.07–1.87)	6	0 (−0.95–0.5)	3
33	SNR	0.27 (−3.09–2.68)	11	0.81 (−1.66–3.28)	6
50	SNR	1.88 (−1.1–9.78)	6	−0.47 (−4.63–1.02)	6
33	CNR	−0.84 (−33.39–31.72)	6	8.46 (−3.5–42.86)	11
50	CNR	27.52 (−9.39–118.84)	6	−0.43 (−27.83–13.19)	6

SD: Standard dose, LD: Low dose, IR: Iterative reconstruction, PS: PixelShine, SNR: Signal-to-noise ratio, CNR: Contrast-to-noise ratio, CL: Confidence limits

The study demonstrated that LD-PS-reconstructed images outperformed LD-FBP images qualitatively and quantitatively. Moreover, LD-PS images were comparable to SD-FBP images. As it is a vendor-neutral software, the addition of the PS algorithm to the older CT scanners with FBP reconstruction will improve the image quality and dose reduction will also be achieved.

The edge sharpness of PS-reconstructed images, though being a denoising reconstruction technique, was not compromised. The interface of the lesion with the adjacent structure was well maintained, hence suitable for clinical diagnosis at lower doses [Figure 8]. In Figure 8 though the PS image appeared smooth, the sub-centimeter-sized lesion conspicuity was maintained with retained shape and margin. This will be especially useful for the evaluation of cases of coarse liver.

In terms of image noise and texture, LD-PS images are equivalent to LD-IR at 50% dose reduction and better than IR as the dose was further lowered to 33% [Figures 9-11]. Hence, in protocols specifically designed for LDs like biopsy procedures, whole-body LD CT for cases like multiple myeloma, or lung cancer screening programs, the PS reconstruction technique has a promising role. Deep-learning-based

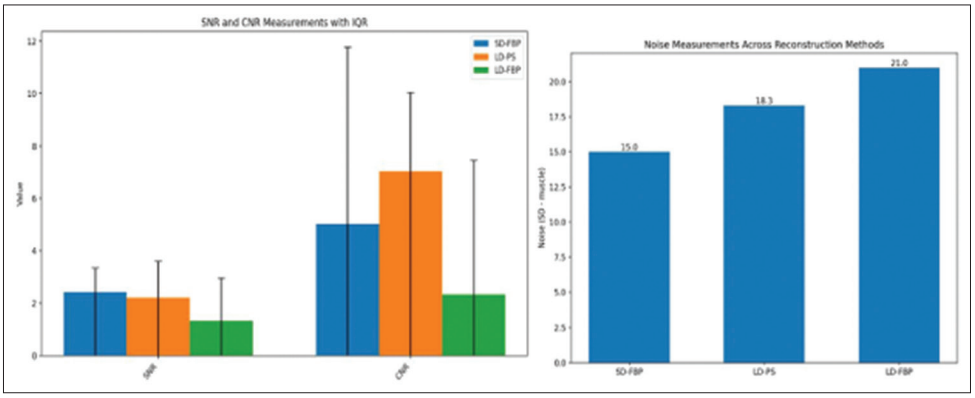

Figure 7: The quantitative results of the parameters of the images ($n = 32$) obtained by Scanner A without any native iterative reconstruction. Low dose = Ranged from 70% to 50% of standard dose. SD: Standard dose, FEP: Filtered back projection, LD: Low dose, PS: PixelShine, IQR: Interquartile range, SNR: Signal-to-noise ratio, CNR: Contrast-to-noise ratio

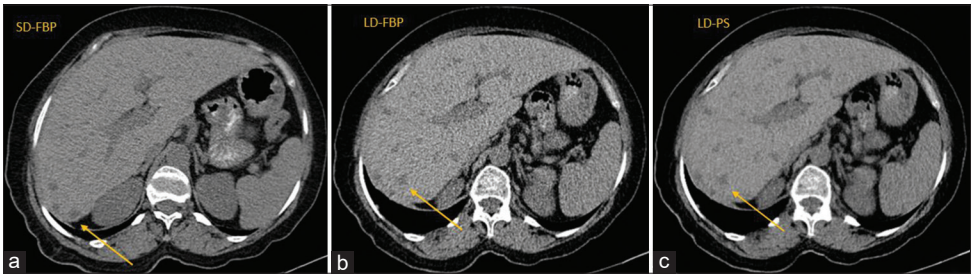

Figure 8: Computed tomography (CT)-guided biopsy procedure performed on scanner A, planning phase scan (a) at standard dose with 260 mA and 110 kV and targeting phase at 50% dose reduction, i.e. 130 mA and 120 kV and low-dose images were reconstructed by filtered back projection (b), and PixelShine (PS) reconstruction (c). PS image shows lower noise (less grainy). Although the image appears smooth, the sub-centimeter-sized liver lesion (arrow) conspicuity is not lost and its margin and shape are maintained. SD: Standard dose, FEP: Filtered back projection, LD: Low dose, PS: PixelShine

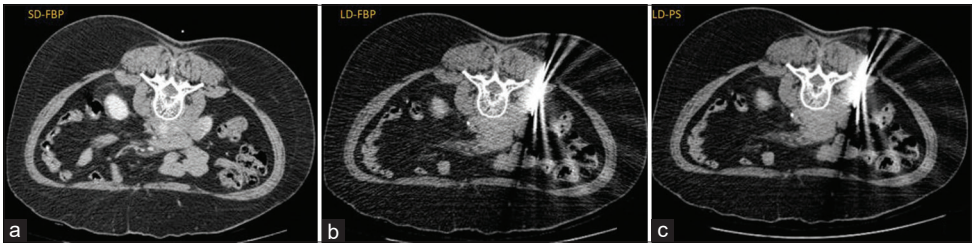

Figure 9: Computed tomography (CT)-guided biopsy procedure was performed on Scanner A with planning phase scan (standard dose) at 334 mA and 120 kV with filtered back projection (FBP) reconstruction (a) and the targeting phase (low dose [LD]) at 160 mA and 120 kV (50% dose reduction). The LD images were reconstructed by FBP (b), and PixelShine (PS) reconstruction (c). PS image has fewer artifacts of the needle and lower magnitude and texture of noise. Needle artifact absent in 9A, as it is a planning phase scan. SD: Standard dose, FEP: Filtered back projection, LD: Low dose, PS: PixelShine

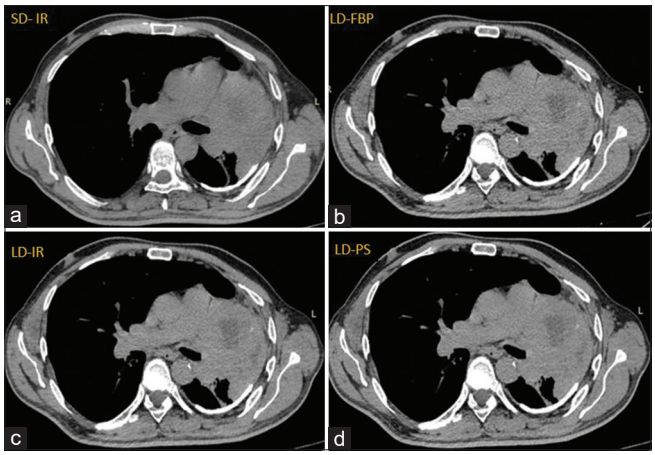

Figure 10: Computed tomography (CT)-guided biopsy procedure performed on Scanner B with native iterative reconstruction (IR) – iDose with planning phase at standard dose (SD) – 237 mA and 120 kV (a) and the targeting phase at approximately 43% of SD, i.e., 104 mA and 120 kV, and low-dose images were reconstructed by filtered back projection (b), IR (c), and PixelShine (PS) reconstruction (d). PS image is less grainy; however, the lesion heterogenicity, margin, and contrast of the necrotic area are maintained. SD: Standard dose, IR: Iterative reconstruction, LD: Low dose, PS: PixelShine, FEB: Filtered back projection

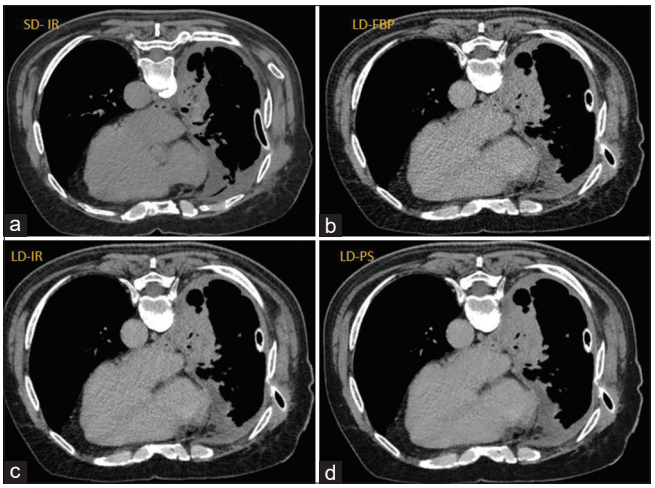

Figure 11: Computed tomography (CT)-guided biopsy procedure performed on Scanner B with native iterative reconstruction (IR) – iDose, planning phase (a) at standard dose (SD) (300 mA and 120 kV) and the targeting phase at 103 mA and 120 kV (30% of SD) and reconstructed by filtered back projection (FBP) (b), IR (c), and PixelShine (PS) reconstruction (d). PS image has lower noise than the FBP and IR images and even the SD image. SD: Standard dose, IR: Iterative reconstruction, LD: Low dose, PS: PixelShine, FEB: Filtered back projection

Table 4: The mean/median bias and points outside bias confidence interval limits in comparison of Standard dose-filtered back projection versus low dose-PixelShine, and low dose-PixelShine versus low dose-filtered back projection images obtained from Scanner A without any native iterative reconstruction (*n*=32)

Dose (percentage of SD mA)	Variable	SD-FBP versus LD-PS		LD-PS versus LD-FBP	
		Mean/median bias (bias CL)	Percentage points outside bias CL	Mean/median bias (bias CL)	Percentage points outside bias CL
50–70	Noise magnitude	0.2 (−0.5–1.5)	0	−0.5 (−1.5–0.07)	3
50–70	Noise texture	0.2 (−0.5–1.5)	0	−0.5 (−1.5–0)	0
50–70	Edge sharpness	0.42 (−0.8–1.65)	6	0 (−0.57–1)	3
50–70	Artifacts	0.26 (−0.86–1.39)	6	−0.4 (−1–1)	0
50–70	Overall score	0.34 (−0.84–1.53)	3	−0.3 (−1.18–0.46)	6
50–70	SNR	−0.02 (−2.12–2.09)	0	0 (−2.07–1.56)	7
50–70	CNR	0 (−14.05–13.23)	7	−0.11 (−15.17–14.71)	7

SD: Standard dose, LD: Low dose, PS: PixelShine, SNR: Signal-to-noise ratio, CNR: Contrast-to-noise ratio, CL: Confidence limits, FBP: Filtered back projection

reconstruction algorithms have been studied, and in areas such as ultra-low-dose pediatric thorax CT, low-dose whole-body CT, and peri-interventional cone-beam CT of the liver, they are found to improve the image quality compared to FBP and hybrid IR techniques with 30% dose reduction.[16-19]

The artifacts were less in PS images compared to IR images at lower doses, 30% of SD [Figures 11 and 12]. The streak artifacts of the bone were less. Being an AI software, there is scope to train the algorithm to reduce the pulsation artifacts of the heart, streak artifacts caused by air in the bowel, and also eliminate the movement artifacts in uncooperative patients.

The evaluation of the lung at 33% of SD mA was not compromised [Figure 13]. Hence, further ultra-low-dose screening programs for lung cancer can be designed.

PS reconstruction technique minimized the artifacts more effectively at lower doses, producing higher quality images. At 33% dose reduction it quantitatively outperformed the IR technique, showing slightly better CNR and SNR. The CNR and SNR of the images at 33% dose reduction were similar to SD-IR images, though the visual impression was lacking. These findings were similar to other studies that show reduced noise and enhanced image SNR and CNR with PS postprocessing.[7,17]

The contrast of the PS images in LD was better [Figures 9 and 11], and lesion heterogenicity was better appreciated. Although artifacts were reduced, this aspect was not compromised.

This study suggests that the PS reconstruction technique offers promising results at a reduced radiation dose in terms

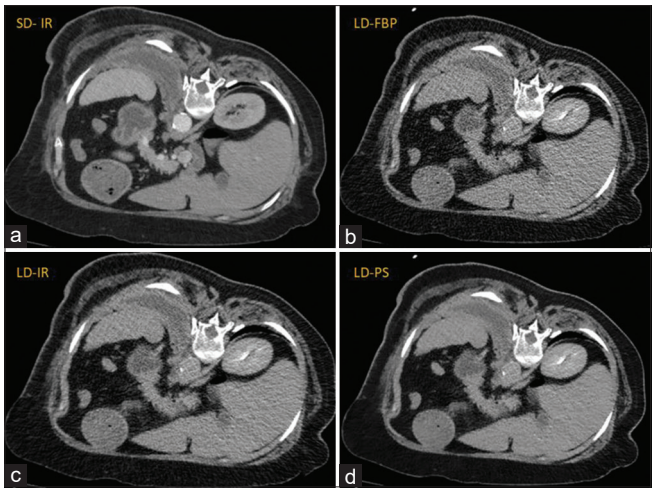

Figure 12: Computed tomography (CT)-guided biopsy procedure performed on Scanner B with native iterative reconstruction (IR) – iDose, planning phase (a) at standard dose (SD) (570 mA and 120 kV) and the targeting phase at 104 mA and 120 kV (30% of SD) and reconstructed by filtered back projection (FBP) (b), IR (c), and PixelShine (PS) reconstruction (d). PS image has lower noise than the FBP and IR images (SD – 12a being a diagnostic scan, the low dose image almost identical to it was selected). SD: Standard dose, IR: Iterative reconstruction, LD: Low dose, PS: PixelShine, FEB: Filtered back projection

of noise and maintains image quality. However, the study had the disadvantage of being a retrospective study with a limited number of patients. Moreover, further reduction in the dose parameters was not explored, and the effect of reduction in kV was not studied.

Further studies are warranted to explore its role and optimize the protocols for different patient populations and diagnostic scenarios like intervention procedures and screening studies.

Conclusions and Future Directions

Conclusion regarding the primary aim

AI-based denoising algorithms such as PS produce very similar and at-par results as that of IR with up to 50% dose reduction. However, with further dose reduction, PS AI significantly outperforms IR, if the exposure is reduced to 33% dose of the standard protocol.

Conclusion regarding the secondary aim

Further reduction at approximately 20% of the original dose may impact diagnostic quality with the current level of AI in PS. Further training of AI with sufficient data availability at significantly low radiation dose levels can improve the diagnostic quality just like other AI. The research may continue in this direction. The conclusion for the secondary objective is that with the use of AI-based reconstructions such as PS, a benchmark of 50% reduction of the original dose of the currently practiced protocols can be safely established.

Miscellaneous conclusions

Mass screening for early detection may demand as much reduction as possible and training the AI over the long term,

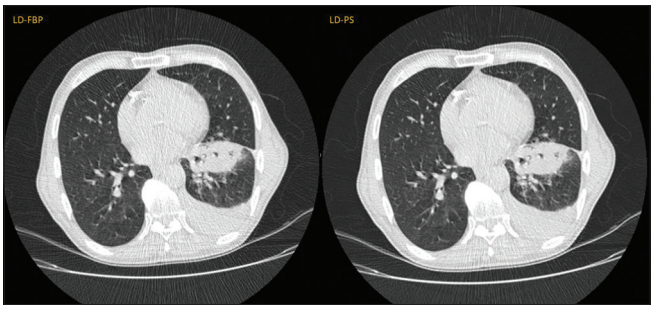

Figure 13: Postprocedure scan was performed at 80 kV and 60 mA and reconstructed with filtered back projection and PixelShine (PS) reconstruction. The low-dose PS image revealed reduced bone artifacts which overlaps the lungs and hence lungs evaluation was not compromised. LD: Low dose, PS: PixelShine, FEB: Filtered back projection

but a 40% reduction in routine diagnostic scans using AI processing post-LD acquisition should be recommended by the regulatory bodies to reduce the exposure hazards significantly.

An indirect benefit of dose reduction is less power dissipation by the X-ray tube of the CT scanner. This is a high-cost consumable of the CT machine, and a separate investigation to establish the benefits of the low-dose CT studies in terms of the following can be performed:

a. The saving in electrical energy and its commercial benefit
b. Extension in the meantime between the failures for the X-ray tube and reduction in the cost of maintenance.

Acknowledgment

I acknowledge Mrs. R. Pallavi, Statistician, Tata Memorial Centre, for her statistical consultant services for this project.

Financial support and sponsorship

Nil.

Conflicts of interest

There are no conflicts of interest.

References

1. Brenner DJ, Hall EJ. Computed tomography – An increasing source of radiation exposure. N Engl J Med 2007;357:2277-84.
2. Nagayama Y, Goto M, Sakabe D, Emoto T, Shigematsu S, Oda S, *et al*. Radiation dose reduction for 80-kVp pediatric CT using deep learning-based reconstruction: A clinical and phantom study. Am J Roentgenol 2022;219:315-24.
3. Pelc NJ. Recent and future directions in CT imaging. Ann Biomed Eng 2014;42:260-8.
4. Power SP, Moloney F, Twomey M, James K, O'Connor OJ, Maher MM. Computed tomography and patient risk: Facts, perceptions and uncertainties. World J Radiol 2016;8:902-15.
5. Nagayama Y, Sakabe D, Goto M, Emoto T, Oda S, Nakaura T, *et al*. Deep learning-based reconstruction for lower-dose pediatric CT: Technical principles, image characteristics, and clinical implementations. Radiographics 2021;41:1936-53.
6. Hornik K, Stinchcombe M, White H. Multilayer feedforward networks are universal approximators. Neural Netw 1989;2:359-66.
7. Tian SF, Liu AL, Liu JH, Liu YJ, Pan JD. Potential value of the PixelShine deep learning algorithm for increasing quality of 70 kVp+ASiR-V reconstruction pelvic arterial phase CT images. Jpn J Radiol 2019;37:186-90.
8. Tian S, Liu A, Pan J, Liu J, Liu Y, Fang X, *et al.* PixelShine algorithm

in enhancing the quality of reconstructed abdominal arterial phase CT image. Chin J Med Imaging 2018;12:205-8.
9. Rozema R, Kruitbosch HT, van Minnen B, Dorgelo B, Kraeima J, van Ooijen PM. Iterative reconstruction and deep learning algorithms for enabling low-dose computed tomography in midfacial trauma. Oral Surg Oral Med Oral Pathol Oral Radiol 2021;132:247-54.
10. Kallianos KG, Elicker BM, Henry TS, Ordovas KG, Nguyen J, Naeger DM. Instituting a low-dose CT-guided lung biopsy protocol. Acad Radiol 2016;23:1130-6.
11. Shepherd TM, Hess CP, Chin CT, Gould R, Dillon WP. Reducing patient radiation dose during CT-guided procedures: Demonstration in spinal injections for pain. Am J Neuroradiol 2011;32:1776-82.
12. Shpilberg KA, Delman BN, Tanenbaum LN, Esses SJ, Subramaniam R, Doshi AH. Radiation dose reduction in CT-guided spine biopsies does not reduce diagnostic yield. Am J Neuroradiol 2014;35:2243-7.
13. Rozema R, Doff MH, van Ooijen PM, Postmus D, Westerlaan HE, Boomsma MF, *et al*. Diagnostic reliability of low dose multidetector CT and cone beam CT in maxillofacial trauma-an experimental blinded and randomized study. Dentomaxillofac Radiol 2018;47:20170423.
14. Niu YT, Mehta D, Zhang ZR, Zhang YX, Liu YF, Kang TL, *et al*. Radiation dose reduction in temporal bone CT with iterative reconstruction technique. Am J Neuroradiol 2012;33:1020-6.
15. Korn A, Fenchel M, Bender B, Danz S, Hauser TK, Ketelsen D, *et al*. Iterative reconstruction in head CT: Image quality of routine and low-dose protocols in comparison with standard filtered back-projection. Am J Neuroradiol 2012;33:218-24.
16. Terzis R, Reimer RP, Nelles C, Celik E, Caldeira L, Heidenreich A, *et al*. Deep-learning-based image denoising in imaging of urolithiasis: Assessment of image quality and comparison to state-of-the-art iterative reconstructions. Diagnostics (Basel) 2023;13:2821.
17. Steuwe A, Weber M, Bethge OT, Rademacher C, Boschheidgen M, Sawicki LM, *et al*. Influence of a novel deep-learning based reconstruction software on the objective and subjective image quality in low-dose abdominal computed tomography. Br J Radiol 2021;94:20200677.
18. Brendlin AS, Plajer D, Chaika M, Wrazidlo R, Estler A, Tsiflikas I, *et al*. AI denoising significantly improves image quality in whole-body low-dose computed tomography staging. Diagnostics (Basel) 2022;12:225.
19. Brendlin AS, Estler A, Plajer D, Lutz A, Grözinger G, Bongers MN, *et al*. AI denoising significantly enhances image quality and diagnostic confidence in interventional cone-beam computed tomography. Tomography 2022;8:933-47.